



EUROfusion

EUROFUSION WPS2-PR(15) 14259

F Warmer et al.

Systems Code Analysis of Helias Fusion Reactor and Economic Comparison to Tokamaks

Preprint of Paper to be submitted for publication in
IEEE Transactions on Plasma Science



This work has been carried out within the framework of the EUROfusion Consortium and has received funding from the Euratom research and training programme 2014-2018 under grant agreement No 633053. The views and opinions expressed herein do not necessarily reflect those of the European Commission.

This document is intended for publication in the open literature. It is made available on the clear understanding that it may not be further circulated and extracts or references may not be published prior to publication of the original when applicable, or without the consent of the Publications Officer, EUROfusion Programme Management Unit, Culham Science Centre, Abingdon, Oxon, OX14 3DB, UK or e-mail Publications.Officer@euro-fusion.org

Enquiries about Copyright and reproduction should be addressed to the Publications Officer, EUROfusion Programme Management Unit, Culham Science Centre, Abingdon, Oxon, OX14 3DB, UK or e-mail Publications.Officer@euro-fusion.org

The contents of this preprint and all other EUROfusion Preprints, Reports and Conference Papers are available to view online free at <http://www.euro-fusionscipub.org>. This site has full search facilities and e-mail alert options. In the JET specific papers the diagrams contained within the PDFs on this site are hyperlinked

Systems Code Analysis of Helias Fusion Reactor and Economic Comparison to Tokamaks

F. Warmer, S.B. Torrasi, C.D. Beidler, A. Dinklage,
Y. Feng, J. Geiger, F. Schauer, Y. Turkin, R. Wolf,
P. Xanthopoulos

Max Planck Institute for Plasma Physics
D-17491, Greifswald, Germany

R. Kemp, P. Knight, H. Lux, D. Ward
Culham Centre for Fusion Energy
Oxfordshire, OX14 3DB, United Kingdom

Contact: Felix.Warmer@ipp.mpg.de

Abstract— Systems codes are commonly employed for the analysis and conceptual design of next-step burning-plasma devices. For the helical-axis advanced stellarator (HELIAS) line a new set of systems code models have been developed to account for the stellarator-specific 3D aspects. The models have recently been implemented in the systems code PROCESS and verified with respect to different test cases.

After having established confidence in the stellarator models, systems studies were carried out for the 5-field period Helias case to define the accessible reactor design window. In the multi-dimensional physics and engineering parameter space sensitivity studies are carried out for the reactor regime to ascertain trade-offs between different parameters and costs. Exemplary design points are analysed in more detail using the plasma operation contour approach which, for example, can be used to determine the Cordey-Pass to ignition.

Finally, with a common set of non-device-specific models, the PROCESS framework allows a direct comparison of tokamaks and stellarators. Although the 5-period Helias is a larger machine in terms of major radius, the required mass for both concepts is comparable leading to similar capital costs.

Keywords—HELIAS, PROCESS, Systems Code, tokamak-stellarator comparison

I. INTRODUCTION

For an assessment of next-step fusion devices, it is not only important to find realistic design points consistent in physics and engineering but also to optimize these design points with respect to the high-level goals and costs. Furthermore, in such a conceptual design phase it is essential to show the robustness of design points with respect to variations in the underlying assumptions. Such a design process is commonly referred to as ‘systems studies’ where engineering and physics parameters are varied to define the accessible reactor design window and to study the sensitivity of the reactor regime considering trade-offs between different parameters and costs.

Such an approach has the advantage of revealing ambiguities in the assumptions which can then be clarified in dedicated experiments and simulations necessary for

identifying critical research paths. Consequently risks and uncertainties are mitigated before the actual engineering design process is started, thereby saving resources which would otherwise be needed for design iterations.

In order to carry out systems studies for next-step fusion devices associated ‘systems codes’ are used which are simplified, yet comprehensive models of an entire fusion power plant. Such an ansatz is well known in the tokamak community and widely used for the assessment of a tokamak demonstration fusion power plant, also known as ‘DEMO’. In this work, for the first time, results of a systems study are presented for the helical-axis advanced stellarator line (HELIAS).

For this purpose stellarator-specific models were developed in [1] designed for a systems code approach consisting of three major models. First, a geometry model to describe the plasma shape (flux surfaces) based on Fourier coefficients. Second, a basic island divertor model for the energy exhaust is derived from geometrical considerations, in addition assuming cross-field transport and radiation at the X-point. And third, a coil model which calculates the maximal field at the coils, the total stored magnetic energy, and the dimensions of the winding pack based on the sophisticated Helias 5-B [2] reactor design where scaling relations and analytic inductance and field calculations are employed in combination with a critical current density scaling of the superconducting material used. For the plasma transport, so far an empirical confinement time scaling for stellarators ISS04 [3] is used but as described in [1] progress has been made in the modeling of plasma transport including neoclassical as well as state-of-the-art turbulence simulations. Limits of confinement enhancement with respect to the empirical ISS04 scaling were investigated in [4].

These HELIAS models were implemented in the systems code PROCESS [5] which is a well-established, partly modular, European tokamak systems code which has gained maturity through years of applications. The implemented stellarator models were verified in detail [6] and showed very good agreement with test cases such as e.g. W7-X providing confidence for the use of the models for HELIAS systems studies. Their implementation in the original tokamak-centric

code PROCESS has the additional advantage that the tokamak and stellarator can be compared within a common framework.

This work is therefore divided into two major parts. The first part, section 2, is dedicated to HELIAS systems studies with emphasis on the general design window analysis and plasma operation contour analysis as well as specific examples such as the effect of tungsten impurities on start-up and plasma operation. The second part, presented in section 3, makes use of the aforementioned common PROCESS framework to compare the tokamak and stellarator, especially economically, for the same set of assumptions and high-level goals. Finally, the work is summarized and the results discussed in section 4.

II. HELIAS SYSTEMS STUDIES

A. Design Constraints and Goals

Before a design window of a HELIAS power plant type device can be outlined several general assumptions must be made about the constraints and goals of such a machine. As the stellarator is an intrinsic steady-state device, the HELIAS power plant aims for an economic base-load power output which must be at least comparable to the level of existing large power plants. Here this will be formulated as a goal to achieve ~1GW net electric power. The production of net electric power is closely interconnected to two other systems of a fusion power plant, namely the power conversion system as well as the blanket structure. Both systems must be conceptually specified for a HELIAS systems analysis.

The power conversion system turning the thermal to electric energy is mainly dependent on the chosen coolant which ultimately determines the thermal conversion efficiency η_{th} . Commonly, the choice is between pressurized water or gaseous helium cooling. The former being a well established technology requiring a moderate amount of pumping power but at a lower efficiency compared to the latter case with higher thermal conversion efficiency but requiring much higher pumping power. A discussion about the detailed pros and cons of both systems is still ongoing in the fusion community. Here, the Brayton power cycle with helium cooling technology has been chosen due to the possibility to work at higher temperatures and to avoid the unresolved safety issues regarding water cooling [7]. Additionally, the higher thermal conversion efficiency, $\eta_{th} = 0.4$, compensates for the higher pumping power, $P_{pump} = 200\text{MW}$, assumed throughout this work [8, 9].

Several different technologies exist also for the blanket composition and its structure. It is beyond the scope of this work to compare the different blanket possibilities and benefits and disadvantages. For this work the dual-coolant (helium and lithium-lead) ferritic steel modular blanket concept was chosen described in [8] compatible with the outlined power conversion system above. The in- and outboard thicknesses are summarized in Tab. 1, where the full blanket thickness is assumed everywhere to ensure a high tritium breeding ratio (TBR) for self-sustained tritium supply.

It should be noted that the above motivated technologies do not represent a final decision but are chosen for a realistic representation of a HELIAS power plant. A decision about the heat conversion and blanket system can only be made after the experimental testing of blanket technologies and detailed assessment of the cooling systems.

TABLE I. MAIN DESIGN PARAMETERS ASSUMED FOR THE HELIAS SYSTEMS STUDIES UNLESS OTHERWISE STATED.

Main design parameters	
Thermal efficiency for He-cooling η_{th}	0.4
Pumping Power for He-cooling [MW]	200
Inboard blanket thickness [m]	0.7
Inboard shield thickness [m]	0.4
Outboard blanket thickness [m]	0.8
Outboard shield thickness [m]	0.7
Superconducting Material	Nb3Sn
HELIAS Field Periods	5
Number of Coils	50

In order to have enough space between the plasma and the coils to accommodate the specified blanket a higher aspect ratio of $A = 12.2$ has been chosen compared to the aspect ratio of $A = 10.5$ in W7-X [10]. The modular coil design and its cross-section are based on [11] where Nb₃Sn is used as superconducting material reflecting the experience gained from ITER.

Throughout this work a 5-field period HELIAS magnetic configuration is chosen because of the more favorable confinement of fast particles and the reduced bootstrap current. A 4-field period configuration may be an option for future investigations as these configurations are further optimized. The lower aspect ratio makes a 4-field period machine a more compact device and may thus be of interest in the future.

The confinement properties of a 5-field period configuration have been investigated in detail [4] where it was found, that the possible confinement enhancement with respect to the empirical confinement time scaling ISS04 [3] depends on different parameters, most notably the size of the machine. For conservative reactor parameters a maximum confinement enhancement factor of $f_{ren} = \tau_E / \tau_E^{ISS04} = 1.5$ was found and serves as upper limit for the presented studies. The empirical confinement time scaling ISS04 is used within the design window analysis of this work and the confinement enhancement factor f_{ren} is iterated with machine size and magnetic field.

According to the 1-D transport simulations with dominating neoclassical transport in the plasma centre and anomalous transport at the plasma edge the volume averaged temperature has been fixed for the HELIAS reactor studies to $\langle T \rangle_v = 7\text{keV}$. The density on the other hand is iterated in the design window analysis to achieve the desired goals such as 1GW net electric power. The radiative density limit, i.e. SUDO-limit [12], observed in some heliotron/stellarator-type devices is not considered in this work since the Large Helical Device (LHD) demonstrated the ability to operate far beyond this limit, especially if pellet injection is used. Therefore the SUDO-limit has been reinterpreted as a density limit for the plasma edge [13, 14]. For the 5-field period case the SUDO-

limit yields a value of $1.6 \cdot 10^{20} \text{m}^{-3}$ which is very high for an edge-limit and thus not relevant for the design window analysis considered here.

Another important aspect of a fusion power plant is the controlled exhaust of energy and particles through the divertor. The model of the island divertor concept consists of a geometrical description including cross-field diffusion and radiation in the SOL and around the X-point [1, 6, 15]. In order to model the island divertor, a set of assumptions need to be taken: For the SOL a perpendicular heat diffusion coefficient of $\chi = 1.5 \text{m}^2/\text{s}$ has been chosen from experimental experience. The inclination between field lines and the divertor target plates was selected to be $\alpha_{\text{lim}} = 2^\circ$ with a field line pitch angle $\Theta = O(10^{-3})$. The temperature in front of divertor is estimated to be $T_t = 3 \text{eV}$ with an effective charge of $Z_{\text{eff}} = 3$ due to the radiating impurities. A heat load limit of $q < 5 \text{MW}/\text{m}^2$ is expected for steady-state reactor conditions and in the following the radiation fraction in the SOL, f_{rad}^* , is varied to fulfill this criterion and will in the design window studies serve as a figure of merit for the exhaust.

As the scenarios investigated in this work concern a burning plasma with production of alpha particles, helium dilution of the plasma must be taken into account. As the particle transport of impurities is not yet fully understood in stellarators a conservative assumption on the helium concentration of 10% has been assumed. This cannot be ignored as helium dilution strongly reduces the fusion power output. Apart from helium no further impurities have been taken into account for the plasma core. Only in the dedicated sensitivity study in section 2.4 have intrinsic tungsten impurities been considered. In future studies other seeded impurities may be taken into account to increase the radiation in the plasma core reducing the power crossing the separatrix and therefore easing the exhaust scenario.

B. Design Window Analysis

Design window analysis has originally been carried out for heliotron reactors as described in [16]. The aim of such an analysis is to define the accessible engineering and physics parameter range for a fusion power plant device respecting specified constraints and goals as described above. For this purpose the main engineering parameters of a HELIAS power plant (the major radius and the magnetic field strength on axis) were systematically varied within a reasonable range ($R = 18 \dots 24$, $B_t = 4.5 \dots 5.6 \text{T}$). In this first study the high-level goals were held constant. That means, in every design point a net electric power of 1GW should be reached. To achieve this while varying the machine size and magnetic field, the plasma density and the confinement enhancement factor were iterated. Two cases are presented in the following, called (A) and (B). In the first case (A) the design window analysis is presented according to the assumptions and goals outlined above. In case (B) only one parameter is changed in comparison to case (A), namely the helium ash concentration in the plasma with a lower value of 5% compared to the 10% in case (A). This has a strong impact on the design window as will be shown in the following explanations.

It should be noted that a single run of a stellarator scenario in PROCESS takes a few minutes on a modern computer. The total calculation time of a 2D-scan as presented in the following is therefore strongly dependent on the chosen resolution. For the design window analysis a 16×16 resolution was chosen which corresponds to ~ 1 day calculation time per figure [17].

1) Case (A)

The results of case (A) are shown in Fig. 1 where isocontours of the volume-averaged plasma beta and the averaged neutron wall load are used as limitations to the design window.

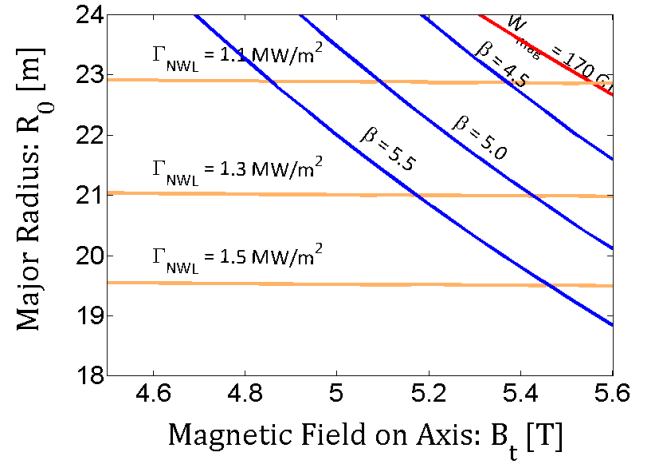


Fig. 1. Case (A): Design window for a HELIAS power plant device with 10% helium concentration constrained to achieve $P_{\text{net,el}} = 1 \text{GW} = \text{const.}$ showing isocontours of the volume-averaged thermal plasma β (blue), the average neutron wall-load (orange), and the stored magnetic energy (red).

As can be seen from Fig. 1 as upper bound a stored magnetic energy of $W_{\text{mag}} = 160 \text{GJ}$ was selected in accordance with [2] in order to keep the stress to components moderate. As the $W_{\text{mag}} = 160 \text{GJ}$ isocontour would coincide with the $\beta = 4.5\%$ contour, $W_{\text{mag}} = 170 \text{GJ}$ is shown in the figure (red line) for clarity. The average neutron wall load (orange lines) is in this analysis not a limiting factor. At a machine size of $R = 23 \text{m}$ the average neutron wall load is rather moderate with $1 \text{MW}/\text{m}^2$. Even a strong reduction of the machine size from 23m to 21m would increase the average neutron wall load only by 20% which is still about a factor two lower than in tokamak reactor studies [18]. However, the plasma beta (blue lines) is a strongly limiting factor in the design window analysis. A conservative beta-limit of 4.5% as predicted by linear stability would lead to a narrow accessible reactor design range. But stellarator experiments have demonstrated the capability to operate above this limit [19, 20, 21, 22] such that beta may be ultimately limited by stochastisation of the plasma edge and corresponding destruction of flux surfaces and shrinking of the plasma volume. Such a beta-limit has been predicted to be in the range of 5 - 6% [23]. As shown in the figure an increase of beta from 4.5 to 5.5% would considerably expand the available

design window. A broader design window allows more freedom to chose a robust design point and further optimize the device with respect to costs, e.g. going to smaller field or machine size for cost reduction.

As already stated in the first case the confinement enhancement factor has been iterated in a conservative way to be in line with [4]. For clarity the associated isocontours of f_{ren} are illustrated separately in Fig. 2. In this figure also the radiation fraction in per cent of the power crossing the separatrix is given which is needed to achieve a peak heat load limit of 5MW/m^2 on the divertor plates.

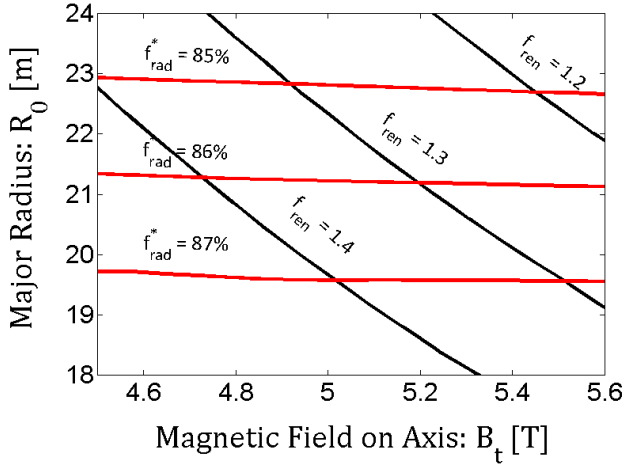


Fig. 2. Case (A): Complement to the design window for a HELIAS power plant device with 10% helium concentration constrained to achieve $P_{\text{net,el}} = 1 \text{ GW} = \text{const.}$ showing isocontours of the confinement enhancement factor f_{ren} (black) and the radiation fraction of the power crossing the separatrix to keep the peak heat load on the divertor plates at 5 MW/m^2 (red).

As can be seen in the complementary Fig. 2 the confinement enhancement factor is conservatively chosen for large machine sizes on the order of $f_{\text{ren}} \sim 1.2$ and increasing for smaller device sizes up to 1.4. The required radiation fraction varies only slightly between 85% - 87%. This is clear as in this design window the net electric power was fixed and thus the alpha heating power and consequently the power crossing the separatrix is nearly constant. Moreover the effective wetted area scales linearly with the major radius and thus changes only from $A_{\text{eff}} = 12\text{m}^2$ for the smallest considered device size up 15m^2 for the maximum size. It should still be noted that a change of the radiation fraction of 1% is in this case equivalent to an additional power of 5MW going directly to the divertor.

2) Case (B)

Analogue to the former case, the results for case (B) are illustrated in Fig. 3 in similar fashion.

As can be seen from the figure the contours of the neutron average wall load do not change in comparison to case (A) as the same fusion power is required to achieve net electric power constraint and therefore the neutron production stays the same. The β -contours on the other hand change considerably and show the strong impact of the helium ash dilution on the plasma performance. This is clear as a higher helium concentrations in the plasma ‘costs’ beta and electron density without increasing the performance.

A complementary figure with contours of the required radiation fraction and the confinement enhancement factor for case (B) is not shown as these parameters are similar to the results presented for case (A) in Fig. 2.

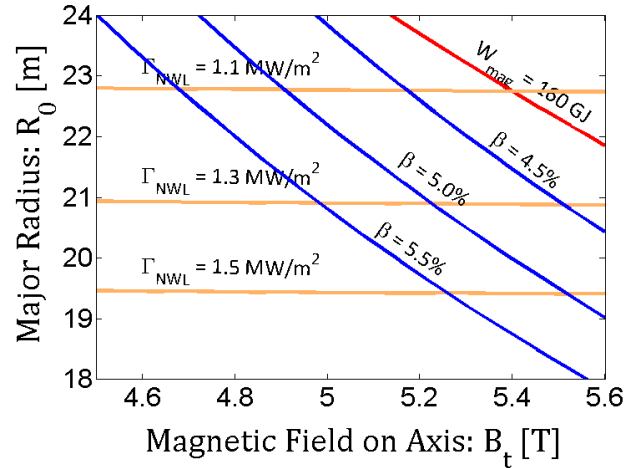


Fig. 3. Case (B): Design window for a HELIAS power plant device with 5% helium concentration constrained to achieve $P_{\text{net,el}} = 1 \text{ GW} = \text{const.}$ showing isocontours of the volume-averaged thermal plasma β (blue), the average neutron wall-load (orange), and the stored magnetic energy (red).

If an operation scenario can be found which effectively flush’s out the helium ash while keeping the confinement for the background plasma high, the size of the machine could be reduced to achieve the same power output or the power output can be increased for the same device size. E.g. if the density profile could be sufficiently controlled one could create a centrally hollow density profile. As the core transport in a stellarator is assumed to be dominated by neoclassical transport, the ambipolarity constraint would give rise to a positive electric field in the plasma centre [24] potentially increasing helium and impurity transport. It is therefore of importance that such advanced scenarios are tested experimentally in W7-X.

Another alternative may be advanced quasi-isodynamic configuration with poloidally closed contours of B which are stable up to $\beta = 7 - 8\%$.

C. Plasma Operation Contour Analysis

In the previous section a design window analysis of the HELIAS was carried out where every point was corresponding to a full reactor concept. Once a suitable design point is found through such a study, it is of interest to further investigate its properties and performance. This can be done by applying Plasma Operation Contour Analysis [25] where density and temperature are varied and the external heating power iterated to reach power balance.

As an example, such a study is presented in the following for the design point with $R = 22\text{m}$, $B_t = 5.5\text{T}$, and a confinement enhancement factor of $f_{\text{ren}} = 1.2$ lying well within the conservative accessible design window outlined by Fig. 1. The volume averaged temperature $\langle T \rangle_v$ and density $\langle n \rangle_v$ has been varied between 3 - 10keV and $0.3 - 3 \cdot 10^{20}\text{m}^{-3}$ respectively. The associated core radiation is assumed to be mainly bremsstrahlung and synchrotron radiation. Only for the tungsten case in section 2.4 additional charge-state-averaged line radiation is included. The results are illustrated in Fig. 4 with isocontours of the required external heating power for power balance shown by the color-coded background.

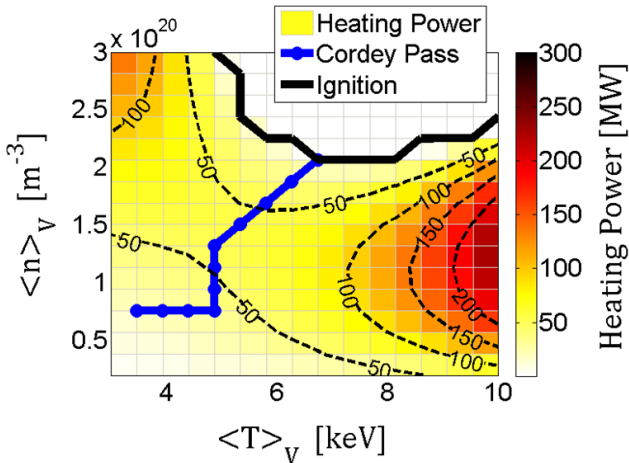


Fig. 4. Plasma Operation Contour Analysis (POPCON) for a HELIAS power plant design point with $R = 22\text{ m}$, $BT = 5.5\text{ T}$, 10% Helium concentration, and $f_{\text{ren}} = 1.2$. Shown in colour-code and isocontours are the external heating power and in blue the Cordey-Pass to the ignition regime (white area).

As is well known and can be seen from Fig. 4 a ‘valley’ of minimum external heating power exists which represents the optimum start-up path considering the minimisation of costs for heating power reserves. This optimum path is illustrated by a blue line and commonly referred to as the ‘Cordey-Pass’. This path ends when the ignition region is reached where the plasma is self-sustained by the alpha heating power, shown as the white region with the black line serving as boundary.

A closer look at this Cordey-Pass can be taken by projection of the associated powers along the steps of this path, illustrated in Fig. 5. Shown are the increasing alpha heating and the increasing radiation while going in the direction of start-up as well as the required heating power

which in this case has a maximum at 55MW. That means, that at least a minimum required heating power (MRHP) of 55MW must be available to achieve plasma start-up.

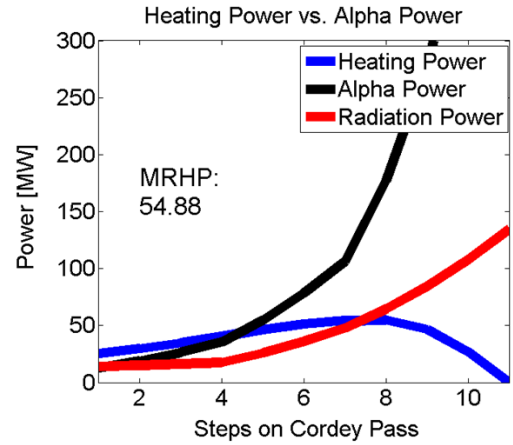


Fig. 5. Projection of the Cordey-Pass from Fig. 4 along its ‘steps’. Shown are the external heating power (blue), alpha heating power (black), and the radiation loss power (red) along this path to ignition with a maximum required heating power of about 55 MW.).

It can be concluded that POPCON plots give insight in the performance of a single design point and the projection of the associated Cordey-Pass allow assessment of the required heating power for start-up. Even for the conservative HELIAS design point investigated here a self-sustained ignition window emerges which can be reached by applying 55MW external heating power.

D. Plasma Operation Sensitivity

Beyond the standard approach to POPCON plots, this analysis can be used for sensitivity studies of a design point against variations in different physics parameters. In the following the influence of two parameters on the plasma operation of our exemplary design point are studied. First is the confinement enhancement factor. An improvement of the confinement leads to reduced plasma power loss through transport at the same plasma energy which consequently leads to a reduced requirement for heating power as less power loss must be compensated. Secondly, the impact of tungsten impurities on the plasma performance is investigated. This is important as a divertor must consist of a resilient material to sustain the strong heat loads for which currently tungsten is foreseen in ITER. But the bombardment of a tungsten metal divertor with energetic particles leads to sputtering and thus tungsten could be an intrinsic impurity in a reactor scenario.

The exemplary design point with $R = 22\text{m}$ and $B_t = 5.5\text{T}$ is varied for two different confinement enhancement factors, namely $f_{\text{ren}} = 1.2$ (top row) as well as $f_{\text{ren}} = 1.4$ (bottom row) as illustrated in Fig. 6. Also the tungsten concentration is changed from $c_w = 0$ (left column) to $c_w = 10^{-5}$ (right column).

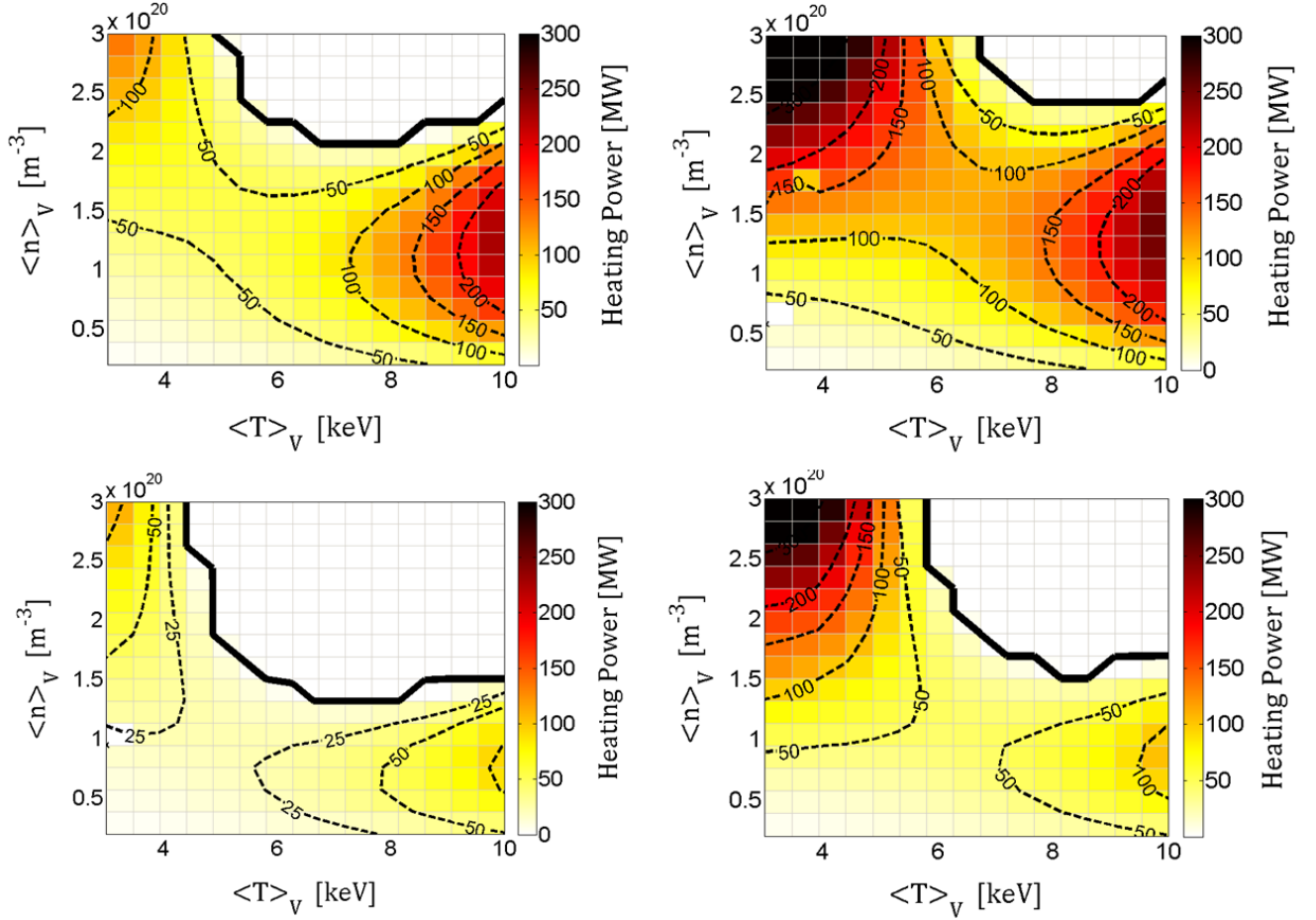


Fig. 6. Plasma operation contour plots are shown with isocontours for external heating power for a HELIAS scenario with $R = 22$ m, $B_T = 5.5$ T, 10% Helium concentration, and a confinement renormalisation factor of 1.2 (top row) as well as 1.4 (bottom row). The left corresponds to cases without tungsten impurities in the plasma and the right to $c_w = 10^{-5}$.

As can be seen from Fig. 6 a moderate increase of confinement not only reduces the required external heating power to reach ignition but also generally increases the whole ignition parameter regime. A self-sustained ignition state is therefore reached at lower temperatures and densities. For the left side without tungsten impurities the required external heating power is reduced from 55MW to 20MW for an increase of the confinement enhancement from 1.2 to 1.4.

If now a moderate tungsten contamination is considered the required external heating power strongly increases compared with the case without tungsten such that in the low-confinement scenario the ignition regime nearly vanishes in the considered parameter region. In this case the required heating power rises to a high value of 120MW while in the high-confinement case the increase to 50MW is tolerable. A closer comparison of the case without and with tungsten impurities also reveals that the impact of the tungsten contamination is greatest in the low temperature regime while the high temperature regime is nearly unchanged. This becomes clear

when the radiative loss function of tungsten is examined which has a strong maximum at 2keV.

From these results it can be concluded that the plasma must be kept free of highly radiating impurities during start-up in order to minimise the required external heating power. In the ignition phase in contrast, a moderate concentration of impurities such as tungsten is tolerable or even favourable. As long as the confinement is not degraded an increase of the core radiation through impurities reduces the power flow to the SOL consequently reducing the demand on the SOL radiation and divertor.

III. COMPARISON TO TOKAMAKS

In order to allow a comparison between tokamak and stellarator the same high-level goals must be applied to both concepts. For this purpose the goals outlined in section 2.1 are adopted for the following tokamak case. That means achievement of 1GW net electric power with helium as coolant for the power conversion system and similar blanket thickness. The H-factor for the confinement enhancement of the tokamak has also been iterated and current drive is used to reach steady-state operation to be comparable to the stellarator. The divertor exhaust cannot be compared as PROCESS currently does not feature a universally accepted tokamak divertor model.

In the first step the design window analysis as presented for the stellarator in section 2.2 is carried out for the tokamak. In this case the major radius and the magnetic field on axis is varied between $R = 6 \dots 9.5\text{m}$, and $B_t = 5.5 \dots 7\text{T}$.

In the next step the costs of both concepts shall be compared. Since every design point in the former analysis represents a whole reactor design with hundreds of parameters each point can be associated with corresponding construction costs. In a design point of PROCESS the size of each component is calculated which is associated with a material. Based on the size of the components and the material densities the total weight for each material can be estimated. With a unit cost per weight the costs of each component are calculated. These are the direct costs of the machine which are complemented by indirect costs which are flat rate of the direct costs depending on the assumed safety level. The PROCESS cost model has been benchmarked with the dedicated cost analysis code FRESKO which showed a reasonable agreement for the total capital costs within 20% [26].

Exemplary design points are selected and compared in a cost-breakdown. For the stellarator again the conservative design point from section 2.3 is used with $R = 22\text{m}$, and $B_t = 5.5\text{T}$. For the tokamak a design point has been chosen similar to the ‘Model B’ of the European PPCS study [18] which lies in the middle of the PPCS parameter range and is therefore neither a too optimistic nor a too pessimistic design point with $R = 8.5\text{m}$, and $B_t = 6\text{T}$. The total construction cost of both these design points have been broken down to their major contributions which are compared in Fig. 7.

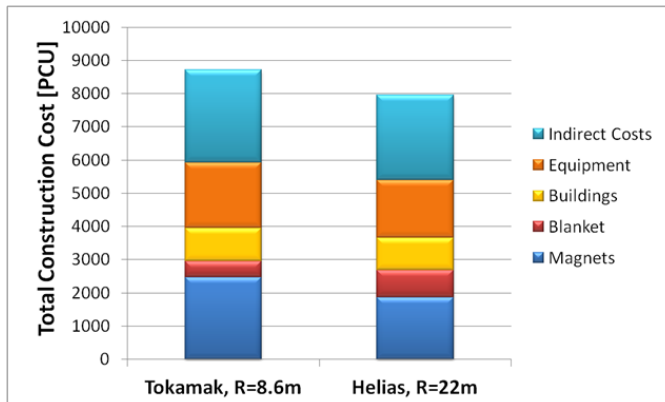


Fig. 7. Cost breakdown of total construction costs to major costing accounts for the selected tokamak and stellarator design point.

As can be seen from Fig. 7 the total magnet costs are higher for the tokamak than for the HELIAS as the massive PF coils add considerable mass of superconducting material (Nb_3Sn) and additional costs for assembly. The blanket cost on the other hand is higher for the HELIAS as the total surface area covered by the blanket is higher due to the higher aspect ratio. This in turn means also that the average neutron wall load is lower in the stellarator ensuring longer lifetime of the exposed inner components. The costs for the buildings are comparable in both the tokamak and stellarator case. The reactor building for the HELIAS must be broader but the tokamak reactor building on the other hand higher while the requirement for other buildings

are similar. The equipment costs, in contrast, are higher for the tokamak as consequence of the requirement for external current drive.

Summarizing, the costs for a tokamak and a HELIAS reactor are comparable for the same set of goals in the common PROCESS framework. Depending on which exact design points are compared construction costs can differ in the range of 10 – 20% for ‘equivalent’ assumptions. The cost-of-electricity (COE) is not investigated in this work. It was already shown in [27] that a variation and statistical sensitivity analysis of different cost factors leads to a non-uniform probability distribution of the COE where the COE with the maximum probability can significantly deviate from the reference value with fixed cost parameters. This is especially important as ambiguities regarding availability and maintenance time and costs exist which have a high impact on the COE. A detailed COE analysis is left for future studies once a better understanding of maintenance schemes is acquired.

IV. CONCLUSIONS

For the first time, a systems code approach has been applied to the helical-axis advanced stellarator line with the aim of defining the accessible design window for a power plant-sized-device. For this, the major radius and the magnetic field on axis were varied over a wide range with the fixed goal to achieve 1GW net electric power. The results from the design window analysis have shown that the accessible design window depends strongly on the envisaged beta-limit. As the beta-limit for HELIAS machines is not yet well specified this results suggests that the beta-limit should be investigated in detail both theoretically and experimentally. The average neutron wall load on the other hand does not limit the design of a HELIAS device as it does not exceed $1.5\text{MW}/\text{m}^2$ even at smaller machine parameters due to the high aspect ratio and surface area. The required confinement enhancement factor with respect to the ISS04 scaling lies between 1.2 - 1.3 for machines of every size at high field which is in line with results from detailed 1D transport simulations. In order to control the power exhaust of such a HELIAS device 85 - 87% of the power crossing the separatrix must be radiated to ensure a peak heat load limit of $5\text{MW}/\text{m}^2$. This may be considered an upper limit as so far only bremsstrahlung and synchrotron radiation were considered in the core, but additional power could potentially be radiated from the core if impurities were to be injected. Even under the most conservative assumptions with $\beta = 4.5\%$ and 10% helium concentration a small feasible design window emerges around $R = 22\text{m}$, $B_t = 5.5\text{T}$. But if a scenario with effective helium exhaust (e.g. hollow density profile) can be found and/or the beta-limit can be verified to be higher, the design window drastically increases opening many more options for potential devices and robust design points. Therefore, it is important that both the beta-limit and hollow density scenarios are in detail investigated in the W7-X experimental campaigns.

Beyond the overarching design-window analysis it was shown that single design points can be further studied using POPCON analysis. Such a detailed study of a single design point shows the ignition window and the path to it which allows determination of the required external heating power which is required to reach the ignition state. Furthermore the POPCON analysis can be used for sensitivity studies. As examples, the impact of the confinement enhancement and the tungsten impurity concentration on the ignition window were studied. It became clear that a higher confinement strongly reduces the required external heating power while increasing the available ignition window. In contrast, an intrinsic impurity concentration of tungsten would make the start-up very difficult as tungsten has a strong radiation maximum at around 2keV while the ignition region at higher temperatures is not affected very much.

Finally the stellarator has been compared to the tokamak concept within the common PROCESS framework. A tokamak design window analysis was carried out for the same set of goals and assumptions and the total construction cost compared. It is an important finding, that the costs for a stellarator are on the same level as the costs for an equivalent tokamak. Although the stellarator is a larger machine in terms of its dimensions, the masses for the different components are comparable to those of a compact tokamak leading in this analysis to similar costs. A detailed cost break-down and comparison of a tokamak and stellarator design point have shown that the costs of the tokamak magnet system is higher due to the high costs for the PF coil system. Also the equipment costs for the tokamak are higher than for the stellarator as the tokamak requires current drive to operate in steady-state which is more cost intensive and also decreases the net efficiency of the concept.

ACKNOWLEDGMENT

Discussions with Prof. A. Sagara and Dr. T. Goto from the National Institute for Fusion Science, Japan, are greatly appreciated.

This work has been carried out within the framework of the EUROfusion Consortium and has received funding from the Euratom research and training programme 2014-2018 under grant agreement No 633053. The views and opinions expressed herein do not necessarily reflect those of the European Commission.

REFERENCES

- [1] F. Warmer, C. D. Beidler, A. Dinklage et al. "HELIAS Module Development for Systems Codes." *Fusion Engineering and Design*, vol. 91, p. 60 (2014).
- [2] F. Schauer, K. Egorov and V. Bykov. "HELIAS 5-B magnet system structure and maintenance concept." *Fusion Engineering and Design*, vol. 88, p. 1619 (2013).
- [3] H. Yamada, J. H. Harris, A. Dinklage et al. "Characterization of energy confinement in net-current free plasmas using the extended International Stellarator Database." *Nuclear Fusion*, vol. 45, p. 1684 (2005).

- [4] F. Warmer, C. Beidler, A. Dinklage et al. "Limits of Confinement Enhancement in Stellarators." *Fusion Science and Technology*, [in press] (2015).
- [5] M. Kovari, R. Kemp, H. Lux et al. "PROCESS: A systems code for fusion power plants - Part I: Physics." *Fusion Engineering and Design*, vol. 89, p. 3054 (2014).
- [6] F. Warmer, C. D. Beidler, A. Dinklage et al. "Implementation and Verification of a HELIAS module for the Systems Code PROCESS." *Fusion Engineering and Design*, [in press] (2014).
- [7] M. Tillack, P. Humrickhouse, S. Malang et al. "The use of water in a fusion power core." *Fusion Engineering and Design*, vol. 91, p. 52 (2015).
- [8] A. R. Raffray, L. El-Guebaly, S. Malang et al. "Engineering Design and Analysis of the ARIES-CS Power Plant." *Fusion Science and Technology*, vol. 54, p. 725 (2008).
- [9] H. Zohm. "On the minimum size of DEMO." *Fusion Science and Technology*, vol. 58, p. 613 (2010).
- [10] G. Grieger and I. Milch. "Das Fusionsexperiment WENDELSTEIN 7-X." *Physikalische Blätter*, vol. 49, p. 1001 (1993).
- [11] F. Schauer. "Coil winding pack FE-analysis for a HELIAS reactor." *Fusion Engineering and Design*, vol. 86, p. 636 (2011).
- [12] S. Sudo, Y. Takeiri, H. Zushi et al. "Scalings of energy confinement and density limit in stellarator/heliotron devices." *Nuclear Fusion*, vol. 30, p. 11 (1990).
- [13] J. Miyazawa, R. Sakamoto, S. Masuzaki et al. "Density limit study focusing on the edge plasma parameters in LHD." *Nuclear Fusion*, vol. 48, p. 015003 (2008).
- [14] L. Giannone, R. Burhenn, K. McCormick et al. "Radiation power profiles and density limit with a divertor in the W7-AS stellarator." *Plasma Physics and Controlled Fusion*, vol. 44, no. 10, p. 2149 (2002).
- [15] Y. Feng. "Up-scaling the island divertor along the W7-stellarator line." *Journal of Nuclear Materials*, vol. 438, p. S497 (2013).
- [16] T. Goto, J. Miyazawa, H. Tamura et al. "Design Window Analysis for the Helical DEMO Reactor FFHR-d1." *Plasma and Fusion Research: Regular Articles*, vol. 7, p. 2405084 (2012).
- [17] S. Torrisi and F. Warmer. "Design of an N-Dimensional Parameter Scanner for the Systems Code PROCESS." Report No. 13/23, Max-Planck-Institute for Plasma Physics (2014).
- [18] D. Maisonnier, D. Campbell, I. Cook et al. "Power plant conceptual studies in Europe." *Nuclear Fusion*, vol. 47, p. 1524 (2007).
- [19] H. Yamada, A. Komori, N. Ohyaibu et al. "Configuration flexibility and extended regimes in Large Helical Device." *Plasma Physics and Controlled Fusion*, vol. 43, no. 12A, p. A55 (2001).
- [20] A. Weller, J. Geiger, A. Werner et al. "Experiments close to the beta-limit in W7-AS." *Plasma Physics and Controlled Fusion*, vol. 45, no. 12A, p. A285 (2003).
- [21] W. A. Cooper, L. Brocher, J. P. Graves et al. "Drift Stabilisation of Ballooning Modes in an Inward-Shifted LHD Configuration." *Contributions to Plasma Physics*, vol. 50, p. 713 (2010).
- [22] K. Ichiguchi and B. A. Carreras. "Multi-scale MHD analysis incorporating pressure transport equation for beta-increasing LHD plasma." *Nuclear Fusion*, vol. 51, no. 5, p. 053021 (2011).
- [23] M. Drevlak, D. Monticello and A. Reiman. "PIES free boundary stellarator equilibria with improved initial conditions." *Nuclear Fusion*, vol. 45, p. 731 (2005).
- [24] F. Warmer. "Reactor Extrapolation of Wendelstein 7-X." Report No. 13/21, Max-Planck-Institute for Plasma Physics (2013).
- [25] W. Houlberg, S. Attenberger and L. Hively. "Contour analysis of fusion reactor plasma performance." *Nuclear Fusion*, vol. 22, no. 7, p. 935 (1982).
- [26] C. Bustreo, G. Casini, G. Zollino et al. "FRESCO, a simplified code for cost analysis of fusion power plants." *Fusion Engineering and Design*, vol. 88, no. 12, pp. 3141 (2013).
- [27] C. Bustreo, T. Bolzonella and G. Zollino. "The Monte Carlo approach to the economics of a DEMO-like power plant." *Fusion Engineering and Design*, [in press], (2015).